energies

MDPI

Article

Long-Term Optimal Scheduling of Hydro-Photovoltaic Hybrid Systems Considering Short-Term Operation Performance

Wenlin Yuan and Zhangchi Sun *

School of Water Conservancy and Transportation, Zhengzhou University, Zhengzhou 450001, China; ywl2009@zzu.edu.cn

* Correspondence: 201703006@stu.ncwu.edu.cn

Abstract: Integrating photovoltaic power stations into large-capacity hydropower stations is an efficient and promising method for regulating large-scale photovoltaic power generation. However, constrained by the time step length, traditional long-term scheduling of hydro-PV hybrid systems does not adequately consider short-term operational performance indicators, resulting in sub-optimal scheduling plans that fail to coordinate the consumption of photovoltaic power and the utilization of water resources in the basin. To address this, this study established a long-term optimal scheduling model for hydro-PV hybrid systems. This model overcomes the limitation of the time step length in long-term scheduling by incorporating long-term power generation goals and short-term operation performance targets into the long-term optimal scheduling process based on scheduling auxiliary functions. In case studies, the optimised model balanced the long-term power-generation goals and short-term operational performance targets by redistributing energy across different periods. Compared to optimization models that did not consider short-term operation performance, in a typical normal year, the model effectively reduced the electricity curtailment volume (28.54%) and power shortage volume (10.91%) of the hybrid system while increasing on-grid electricity (0.03%). Similar improvements were observed in wet and dry years. These findings provide decision support for hydropower scheduling in the context of large-scale photovoltaic power integration.

Keywords: cascade hydropower stations; hydro-PV hybrid system; long-term optimal scheduling; multi-objective optimization; energy production

check for updates

Citation: Yuan, W.; Sun, Z. Long-Term Optimal Scheduling of Hydro-Photovoltaic Hybrid Systems Considering Short-Term Operation Performance. *Energies* **2024**, *17*, 5388. https://doi.org/10.3390/en17215388

Received: 4 October 2024
Revised: 25 October 2024
Accepted: 26 October 2024
Published: 29 October 2024

Copyright: © 2024 by the authors. Licensee MDPI, Basel, Switzerland. This article is an open access article distributed under the terms and conditions of the Creative Commons Attribution (CC BY) license (https://creativecommons.org/licenses/by/4.0/).

1. Introduction

As the global energy supply tightens and ecological degradation intensifies, the limitations of traditional fossil fuels, particularly their high carbon emissions, have become increasingly evident [1]. Thus, accelerating the development and utilization of renewable energy sources (RESs) and achieving the green and low-carbon transformation of energy systems have become major strategic measures to ensure energy security and achieve high-quality development [2,3]. Among common RESs, photovoltaic (PV) power generation has a substantial development potential because the technology is mature, widely distributed, and the operational and maintenance costs are low [4]. However, PV power generation is highly volatile and intermittent [5], and it lacks inherent regulation capabilities that directly integrate it into the grid, thus posing challenges to grid operational stability. Integrating PV power generation with controllable power sources such as hydropower [6], pumped-storage hydropower [7], and energy storage facilities [8,9] into hybrid energy systems can effectively offset the high variability of photovoltaic power stations, resulting in a relatively stable electrical energy output. Large-scale hydropower stations, with their excellent regulatory capabilities, can respond swiftly to PV fluctuations, making their integration with PV power an efficient and promising method for regulating large-scale PV power generation [10,11]. In addition, the use of hydropower, which is a clean power source, is rapidly increasing in scale globally. If we can harness its electrical energy while fully leveraging its

excellent regulatory capabilities to mitigate the uneven output of photovoltaic and wind power sources [12], it would undoubtedly lead to improved economic and social benefits.

To address the long-term scheduling of hydro-PV hybrid systems, numerous insightful explorations have been conducted based on traditional hydropower scheduling incorporating long-term complementary operational characteristics. In this respect, Cao et al. [13] utilised the solar radiation and inflow sequences generated by the scenario tree (ST) method as inputs for an optimal reservoir operation model, and proposed a multistage rolling reservoir decision model that accounted for uncertainties in solar radiation and inflow. Li et al. [14] established a multi-objective optimization model to maximise total energy production and guaranteed rates and conducted a study to enhance the long-term complementary operational performance of large-scale hydro-PV hybrid power plants. Lu et al. [15] proposed an improved interval optimization method for modelling uncertainties in the inflow runoff of cascade hydropower plants and PV power output. Li et al. [16] proposed a multi-objective optimization model aimed at developing a long-term balanced operational plan for hydro-PV power systems in consideration of the grid's benefits, stability, and tolerance, and a series of reservoir operational schemes was presented based on an analysis of the competitive relationships among the objectives. However, all these studies primarily targeted long-term scheduling on monthly or ten-day scales, and they insufficiently considered the short-term operational performance [17,18], making it difficult for the resulting long-term optimal dispatch scheme to effectively coordinate PV energy grid integration with the integrated use of water resources in the basin [19,20].

Effective methods for optimising the short-term operational performance of hydro-PV hybrid systems have been developed, and such studies primarily focus on PV output uncertainty [21,22], complementary scheduling modelling [23–25], and efficient models for solving scheduling models [26–29]. In this respect, Park et al. [22] studied the correlation among cloud cover, solar irradiance, and estimated solar power output by predicting solar irradiance. In addition, Yuan et al. [23] proposed a practical coordination mode between a PV plant and a large-capacity hydropower plant based on a negotiation mechanism between the power generation company and the power grid. Furthermore, several linearization methods have been introduced to transform the original model into a scenario-based mixed-integer linear programming problem to obtain optimal solutions. Inspired by the game of musical chairs, Eltamaly [26] designed the Musical Chairs Algorithm, which they applied to the parameter estimation of photovoltaic cells. Although this new type of algorithm has not been applied in reservoir scheduling to date, its strong advantages have already been evidenced. Acknowledging the limitations of traditional stochastic optimization and robust optimization approaches, Zhang et al. [28] tailored a joint optimization dispatching method for a cascaded hydro-PV–pumped-storage hybrid system based on data-driven distributionally robust optimization. These short-term optimization models typically use hourly or shorter time steps to account for the intraday variability of the PV output or load demand; however, when applied to study the long-term operation of hydro-PV hybrid systems, they result in decision variable scales of tens to hundreds of thousands, imposing a heavy computational burden. Therefore, to accommodate large-scale PV integration into hydropower scheduling, several long-term optimization scheduling models that consider short-term operational performance have been proposed and studied. Guo et al. [30] constructed a complementary short-term optimization scheduling model under long-term scheduling boundary conditions and simulated daily power generation planning and real-time operation to calculate the corresponding PV curtailment rates for a cost-benefit analysis of PV power stations. However, their study failed to demonstrate the influence of short-term scheduling results on long-term scheduling operations. Ming et al. [31] quantified the short-term operational performance indicators of hydro-PV hybrid systems within long-term scheduling periods based on daily scheduling models and derived adaptive scheduling rules for a complementary system. However, the representativeness of short-term scheduling scenarios of such models has not yet been determined. Therefore, unlike

the aforementioned studies, the current study focuses on demonstrating how short-term scheduling scenarios are determined to ensure their representativeness.

This study aimed to establish a long-term optimal scheduling model for hydro-PV hybrid systems considering the short-term operational performance. Specifically, we aimed to (1) construct scheduling auxiliary functions to represent the long-term hydropower output and short-term performance indicators, and (2) evaluate the trade-offs between long-term power generation and short-term operational objectives to develop an optimal operation scheme. This model addresses the limitations of traditional long-term scheduling by balancing long-term power generation objectives with short-term operational performance objectives based on scheduling auxiliary functions extracted from a multi-scenario analysis of short-term simulation scheduling results from different scenarios.

The remainder of this paper is organised as follows: Section 2 provides a detailed description of the long-term optimal scheduling model for hydro-PV hybrid systems based on scheduling auxiliary functions. It also provides the extraction steps for scheduling auxiliary functions, describes the model solution method, and introduces a case study based on the Wu River hydro-PV hybrid system in China. Section 3 discusses the results of this case study; and Section 4 summarises the study.

2. Materials and Methods

To maximise long-term on-grid electricity while optimising short-term operational performance indicators, we employed auxiliary scheduling functions to integrate the short-term operational capabilities of the hydro-PV hybrid system into the optimisation principles of the long-term scheduling model. This established a long-term multi-objective optimal scheduling model for a hydro-PV hybrid system. To derive the scheduling auxiliary functions, significant influencing factors, such as the initial water level, inlet flow, and PV power output of the system, were considered. A series of typical daily scenarios were established to simulate the short-term operation processes of these scenarios, and the simulation results were analysed to obtain quantitative representations of the relationship between the long-term hydropower output and short-term operation performance indicators for the hydro-PV hybrid system that served as auxiliary scheduling functions. Finally, the multi-objective optimization scheduling model was solved, and a balanced solution was selected from the resulting Pareto optimal solution set using a fuzzy multi-attribute decision-making approach that served as the recommended scheduling scheme. The overall framework of this approach is illustrated in Figure 1. In this methodology, the scheduling auxiliary functions were first derived. Long-term scheduling requires a monthly time step, within which the short-term operational performance indicators considered are realized through the scheduling auxiliary functions.

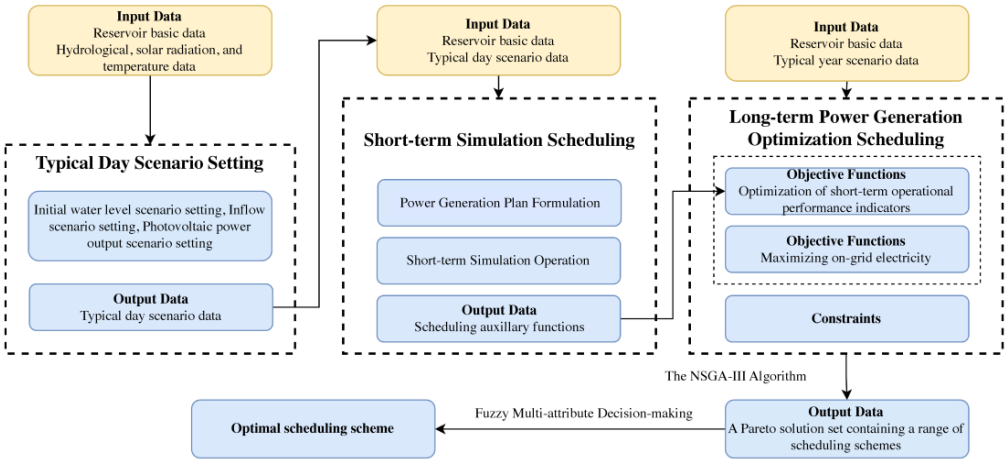

Figure 1. Research framework for studying the long-term optimal scheduling of hydro-PV hybrid systems and considering the short-term operation performance.

2.1. Long-Term Optimal Scheduling Model for Power Generation

2.1.1. Objective Functions

This study focused on the power-generation performance of a hydro-PV hybrid system. Two indices, the electricity curtailment rate and power shortage rate, defined as the ratios of the electricity curtailment volume to the generated electricity and power shortage volume to the generated electricity, respectively, were adopted to characterise the short-term operation performance of the hybrid system. These values at the t-th time period are denoted as $EC(t)$ and $PS(t)$. In the objective function, the goal regarding the short-term operational performance indicators of the hybrid system is to minimize the electricity curtailment volume and power shortage volume during the scheduling period; Owing to the existence of electricity curtailment, the long-term power generation target should be to maximise electricity generation (i.e., maximizing the on-grid electricity), which are defined by the following equations:

(1) Maximizing on-grid electricity

$$F_1 = max\sum_{t=1}^{T}[1 - EC(t)]\cdot[N_h(t) + N_{pv}(t)]\cdot\Delta t, \quad (1)$$

$$N_h(t) = \sum_{i=1}^{I} N_{h,i}(t), \quad (2)$$

where F_1 is the on-grid electricity of the hybrid system throughout the entire scheduling period; $N_h(t)$ and $N_{pv}(t)$ are the total output of the cascade hydropower plants and the output of the PV power plant, respectively, in time period t; $EC(t)$ is the average electricity curtailment rate in time period t; T is the number of long-term scheduling periods; Δt is the time step of the long-term scheduling; $N_{h,i}(t)$ is the output of the ith hydropower station in the cascade in time period t; and $i \in [1, N]$, where N is the number of cascade reservoirs.

(2) Minimizing the electricity curtailment volume

$$F_2 = min\sum_{t=1}^{T} EC(t)\cdot[N_h(t) + N_{pv}(t)]\cdot\Delta t \quad (3)$$

where F_2 is the electricity curtailment volume for the entire scheduling period.

(3) Minimizing power shortage volume

$$F_3 = min\sum_{t=1}^{T} PS(t)\cdot[N_h(t) + N_{pv}(t)]\cdot\Delta t \quad (4)$$

where F_3 is the power shortage volume for the entire scheduling period and $PS(t)$ is the average power shortage rate in time period t.

2.1.2. Constraints

(1) Water balance constraints:

$$V_i(t) = V_i(t-1) + [Q_i(t) - q_i(t)]\cdot\Delta t \quad (5)$$

where $V_i(t)$ is the reservoir storage volume of the i-th hydropower station in time period t, and $Q_i(t)$ and $q_i(t)$ are the inlet and discharge flows of the i-th hydropower station in time period t, respectively.

(2) Hydraulic connection constraints:

$$Q_{i+1}(t) = q_i(t) + R_i(t) \quad (6)$$

where $R_i(t)$ is the interval flow between the ith and $(i + 1)$-th hydropower stations during period t.

(3) Water level–storage capacity relationship constraints:

$$Z_i(t) = f_i^{zv}[V_i(t)] \tag{7}$$

where $Z_i(t)$ is the reservoir water level of the i-th hydropower station during time period t and $f_i^{zv}(\cdot)$ is the water level–storage capacity relationship for the i-th hydropower station.

(4) Tailwater level–discharge flow relationship constraints:

$$Z_{tail,i}(t) = f_i^{zq}[q_i(t)] \tag{8}$$

where $Z_{tail,i}(t)$ is the tailwater level of the i-th hydropower station during time period t and $f_i^{zq}(\cdot)$ is the relationship between the tailwater level and the discharge flow for the i-th hydropower station.

(5) Water level constraints:

$$Z_{i,min}(t) \le Z_i(t) \le Z_{i,max}(t) \tag{9}$$

where $Z_{i,min}(t)$ and $Z_{i,max}(t)$ are the lower and upper limits of the reservoir water level of the ith hydropower station during time period t, respectively.

(6) Boundary condition constraints:

$$Z_i(0) = Z_{i,start}, \tag{10}$$

$$Z_i(T_s) = Z_{i,end}, \tag{11}$$

where $Z_i(0)$ is the reservoir water level of the i-th hydropower station at the beginning of the first time period, $Z_i(T_s)$ is the reservoir water level of the i-th hydropower station at the end of the $T_s -$ th time period, and $Z_{i,start}$ and $Z_{i,end}$ are the specified initial and final water levels for the i-th hydropower station, respectively.

(7) Discharge flow constraints:

$$q_{i,min}(t) \le q_i(t) \le q_{i,max}(t) \tag{12}$$

where $q_{i,min}(t)$ and $q_{i,max}(t)$ are the lower and upper limits of the discharge flow of the ith hydropower station during time period t, respectively.

(8) Hydropower output constraints:

$$N_{h,i}^{min}(t) \le N_{h,i}(t) \le N_{h,i}^{max}(t) \tag{13}$$

where $N_{h,i}^{min}(t)$ and $N_{h,i}^{max}(t)$ are the upper and lower limits of the output value of the i-th hydropower station during time period t and $N_{h,i}(t)$ is the output of the hydropower station(s) during time period t.

(9) Non-negative constraints

This model imposes non-negative constraints on all variables, ensuring that they are not less than zero.

2.2. Scheduling Auxiliary Functions

Hydroelectricity is complementary to PV power generation because of its flexibility; however, this flexibility is not static. A statistical analysis of the short-term operational results of a series of complementary systems can quantitatively characterise the correlation between the hydropower output and short-term operational performance indicators over long-term scheduling periods [32]. Therefore, we constructed two scheduling auxiliary functions that reflected the relationship between two short-term operational performance

indicators (the electricity curtailment rate and the power shortage rate) and long-term hydropower output, as follows:

$$EC(t) = f^{ec}[N_h(t)] \tag{14}$$

$$PS(t) = f^{ps}[N_h(t)] \tag{15}$$

where $f^{ec}(\cdot)$ and $f^{ps}(\cdot)$ are the auxiliary functions for electricity curtailment and power shortage, respectively.

Based on a multi-scenario analysis of a short-term simulation scheduling model, the following steps were performed to extract the scheduling auxiliary functions:

Step 1: Scenario setting. Various scenarios were considered for the initial water levels of the reservoirs, inflow, and PV power generation outputs across different scheduling periods in the cascade system. These scenarios were combined to obtain a series of representative daily scenarios (see Section 2.2.1).

Step 2: Short-term simulation scheduling. A short-term optimal scheduling model for the hydropower-PV complementary system was established and the short-term operational processes of the complementary system under each typical daily scenario were solved (Section 2.2.2).

Step 3: Extraction of auxiliary scheduling functions. First, the hydropower output, electricity curtailment rate, and power shortage rate were calculated for each typical daily scenario. Subsequently, suitable functions were fitted to the optimization results of the hydropower output and electricity curtailment rate to extract the functional relationship between the hydropower output and the electricity curtailment rate $f^{ec}(\cdot)$. The functional relationship between the hydropower output and the power shortage rate $f^{ps}(\cdot)$ was also extracted using the aforementioned method.

2.2.1. Scenario Setting

Based on a series of typical day scenarios, we extracted a scheduling decision function from the short-term simulation scheduling results. Therefore, the representativeness of the typical day scenarios directly determines the representativeness of the extracted scheduling decision function. To ensure the representativeness of the typical day scenarios, we considered various scenarios in terms of the initial water levels, available water volumes, and the PV output over different long-term scheduling periods, and we then combined these scenarios to simulate the various situations that may arise in short-term scheduling within each long-term period. The scenarios used are as follows:

(1) Initial water levels

The initial water level of the cascade reservoirs influences the daily operational tactics of the hydro-PV integrated system. In this study, diverse scenarios were established based on the high and low water marks of the peak and trough water levels attainable by individual reservoirs across various dispatch periods throughout the year. When dealing with issues related to cascade reservoirs, a reservoir located upstream with a good regulation performance, a longer regulation cycle, and a larger proportion of the system's regulation capacity was selected as the "leading" reservoir in the cascade. When setting the water level scenarios, it was assumed that the water levels of all reservoirs in the cascade were synchronised with the "leading" reservoir. When setting the initial water-level scenarios, all long-term scheduling periods were divided into flood and non-flood seasons. For non-flood scheduling periods, several groups of scenarios were evenly set between the flood limit level and the dead water level of the "leading" reservoir; other reservoirs also set scenarios evenly between their flood limit levels and dead water levels based on the principle of "high water level corresponds to high water level, low water level corresponds to low water level." For flood scheduling periods, based on the above operations, additional groups of scenarios were set between the design flood level and the flood limit level of each reservoir.

(2) Available water volume (inflow)

On a typical day, the volume of water utilised for power generation is directly correlated with the amount of electricity produced, thereby exerting a notable influence on the short-term operational tactics of the hydro-PV hybrid system. From a short-term perspective, the available water volume for a typical day is given by long-term scheduling, whereas from a long-term perspective, with the exception of a few reservoirs with special operational requirements, the distribution of a reservoir's outflow can be measured by the inflow distribution. We considered the inflow of a typical day's scenario as the available power generation flow and established several groups of scenarios based on the hydrological frequency of the inflow. The daily average inflow data for each long-term scheduling period were grouped and the daily average inflow (or interval flow) corresponding to the different hydrological frequencies of each scheduling period were calculated using the fitting line method. As the runoff characteristics at different stations and intervals differed in the same river, the flow data that appeared simultaneously in different reservoirs did not entirely have the same frequency. Therefore, when setting the inflow scenarios of cascade reservoirs in this paper, the hydrological frequency of the inflow of the "leading" reservoir in the cascade was used as the standard.

(3) PV output

Uncertainty in PV output forecasting poses risks to executing the complementary system of the given power generation plan. Therefore, we used Latin hypercube sampling to generate several groups of PV output scenarios for each PV output forecasting process to simulate the uncertainty of PV output forecasting in reality. For a certain PV output forecasting process N_{pv}, we considered several PV output scenarios to characterise the uncertainty of PV output forecasting, where the k-th PV output scenario is denoted as $N_{pv,k}$.

(4) Scenario combinations

Each set of typical day scenarios included the initial water levels of the cascade reservoirs, the inflow or interval flow of the cascade reservoirs, the PV output forecasting processes, and the PV output scenarios. To reduce the computational burden, a PV output forecasting process was considered during a long-term scheduling period. Assuming that a long-term scheduling period has A initial water level scenarios, B inflow scenarios, and C PV output scenarios, the total number of typical day scenarios for that long-term scheduling period is $A \cdot B \cdot C$, as shown in Figure 2.

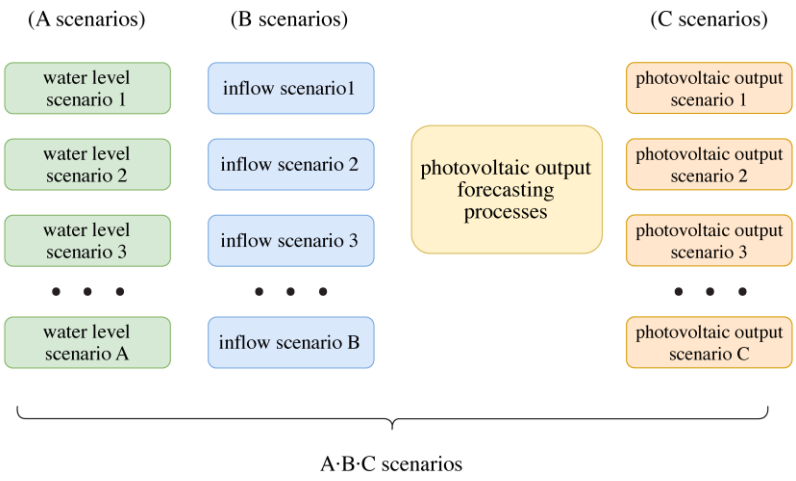

Figure 2. Scenario setting illustration.

2.2.2. Two-Stage Short-Term Simulation Scheduling

The short-term simulation scheduling of the hydro-PV hybrid system comprehensively considers the various short-term characteristics of hydropower, such as the inflow

process and PV power (such as the PV power output process), thereby enabling the precise simulation of scenarios involving electricity curtailment and power shortages. Typically, the prediction of inflow is relatively accurate within a one-day forecast horizon; however, within the same forecast horizon, the prediction of PV output has strong uncertainty [33]. Based on this, we assumed that the prediction of inflow was accurate, and we mainly studied the risk associated with the uncertainty of PV output prediction in the execution of a given power generation plan of one complementary system. In the process of hydropower regulating the fluctuations in PV output, an actual output lower than the generation plan will cause a power shortage, whereas an actual output higher than the generation plan will cause electricity curtailment [34], as shown in Figure 3.

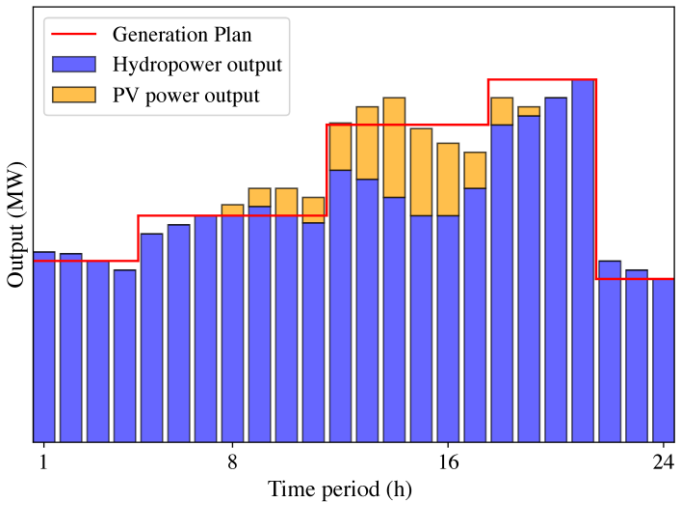

Figure 3. Schematic diagram of electricity curtailment and power shortage in hydro-PV hybrid systems.

Short-term simulation scheduling of the hydro-PV hybrid system includes two stages: power generation plan formulation and short-term simulation operation. First, based on the power generation capacity of the hydro-PV hybrid system and the demand for the power system, a power generation plan curve was formulated for the complementary system [35]. Then, considering the uncertainty of PV output prediction, the process of cascade hydropower regulating the fluctuations of PV output was simulated according to the formulated power generation plan curve. The objective function of the power generation plan formulation stage minimises the standard deviation of the remaining load, and that of the short-term simulation operation stage minimises the total load deviation. Considering the k-th PV output scenario as an example, the following equations were used:

(1) Power generation plan formulation

$$G_1 = min\sqrt{\frac{\sum_{t=1}^{T_s}[L^{re}(m) - \overline{L^{re}}]^2}{T_s}} \tag{16}$$

$$L^{re}(m) = L(m) - N_p(m) \tag{17}$$

$$N_p(m) = N_h(m) + N_{pv}(m) \tag{18}$$

where T_s is the number of short-term scheduling periods, $L(m)$ is the load of the main power grid during period m, $N_p(m)$ is the power generation plan for the complementary system during period m, $L^{re}(m)$ is the residual load during period m, $\overline{L^{re}}$ is the arithmetic mean of the residual load, $N_h(m)$ is the hydropower output during period m, and $N_{pv}(m)$ is the predicted PV output for period m.

(2) Short-term simulation

$$G_2 = min \sum_{m=1}^{T_s} \left| N_{h,k}(m) + N_{pv,k}(m) - N_p(m) \right| \quad (19)$$

where $\Delta N_k(m)$ is the deviation between the actual output and the generation plan of the complementary system during period m under the k-th PV output scenario, $N_{h,k}(m)$ is the hydropower output of the cascade system during period m in the studied scenario, and $N_{pv,k}(m)$ is the PV output during period m in the studied scenario.

The constraints of the short-term simulation scheduling model include water balance constraints, hydraulic connection constraints, water level constraints, boundary condition constraints, outflow constraints, hydropower output constraints, and non-negativity constraints, which are not elaborated on further here.

2.2.3. Extraction of Scheduling Auxiliary Functions

First, the hydropower output, electricity curtailment rate, and power shortage rate corresponding to each typical day scenario were employed, taking the k-th PV output scenario as an example:

$$N = \frac{1}{T_s} \cdot \sum_{m=1}^{T_s} N_{h,k}(m) \quad (20)$$

$$EC = \frac{\sum_{m=1}^{T_s} \Delta N_k(m) \cdot \Delta t_s}{\sum_{m=1}^{T_s} N_p(m) \cdot \Delta t_s}, \ \Delta N_k(m) > 0 \quad (21)$$

$$PS = \frac{\sum_{m=1}^{T_s} -\Delta N_k(m) \cdot \Delta t_s}{\sum_{m=1}^{T_s} N_p(m) \cdot \Delta t_s}, \ \Delta N_k(m) < 0 \quad (22)$$

$$\Delta N_k(m) = N_{h,k}(m) + N_{pv,k}(m) - N_p(m) \quad (23)$$

where N is the average hydropower output for the typical day scenario, $N_{h,k}(m)$ is the output of the cascade hydropower stations during period m for the typical day scenario, and EC and PS are the average electricity curtailment rate and average power shortage rate, respectively, for the typical day scenario.

Sequences were then formed with the hydropower output and electricity curtailment rate, as well as the hydropower output and power shortage rate. Nonlinear fitting methods were used to fit the functional relationships between hydropower output and the electricity curtailment rate, and between hydropower output and the power shortage rate, thereby extracting the scheduling auxiliary functions $f^{ec}(\cdot)$ and $f^{ps}(\cdot)$.

2.3. Model Solution Method

2.3.1. Non-Dominated Sorting Genetic Algorithm II (NSGA-III)

The non-dominated sorting genetic algorithm II (NSGA-II) in multi-objective intelligent algorithms is widely used to solve multi-objective reservoir scheduling models owing to its short optimization time and good optimization effect [36]. However, the NSGA-II selects individuals within the same non-dominated level based on crowding distance, and its convergence and diversity performance are not satisfactory for solving multi-objective problems (MaOPs). To apply genetic algorithms in MaOPs, Deb [37] proposed a multi-objective genetic algorithm based on a reference point selection mechanism, namely, the non-dominated sorting genetic algorithm III (NSGA-III). This algorithm uses a reference point-based selection method that is more efficient and accurate for solving MaOPs [38]. The optimization scheduling model established in this study is a typical many-objective problem; hence, the NSGA-III was chosen to solve the scheduling model established in this study. The discharge flow of each power station for each period was considered the decision variable, and a series of scheduling schemes (i.e., individuals) were generated

based on the constraints of the discharge flow. Each scheduling scheme can be represented by Equation (24):

$$Cr_p = \{q_1(1), q_1(2), \ldots, q_1(T), q_2(1), \ldots, q_N(T)\}_p \quad (24)$$

where Cr_p is the p-th scheduling scheme, $q_1(T)$ is the discharge flow of the first reservoir in the cascade during the T-th period, and the other symbols are the same as those previously defined.

The end-of-period storage for each reservoir was then calculated and the end-of-period water level was determined based on the water level–storage curve. From this, the power generation process of each power station was obtained, and combined with the objective function, the fitness of each scheduling scheme was calculated. Non-dominated sorting was performed and divided into non-dominated layers, ensuring that all solutions within each layer were mutually non-dominated and dominated all solutions in the next layer. They sequentially underwent selection, crossover, and mutation operations to obtain a new generation of better fitness indicators. The above steps were repeated, and when the number of iterations reached the set maximum value, the individuals of the first non-dominated layer (i.e., the Pareto solution set) were the final result. The complete solution process is illustrated in Figure 4.

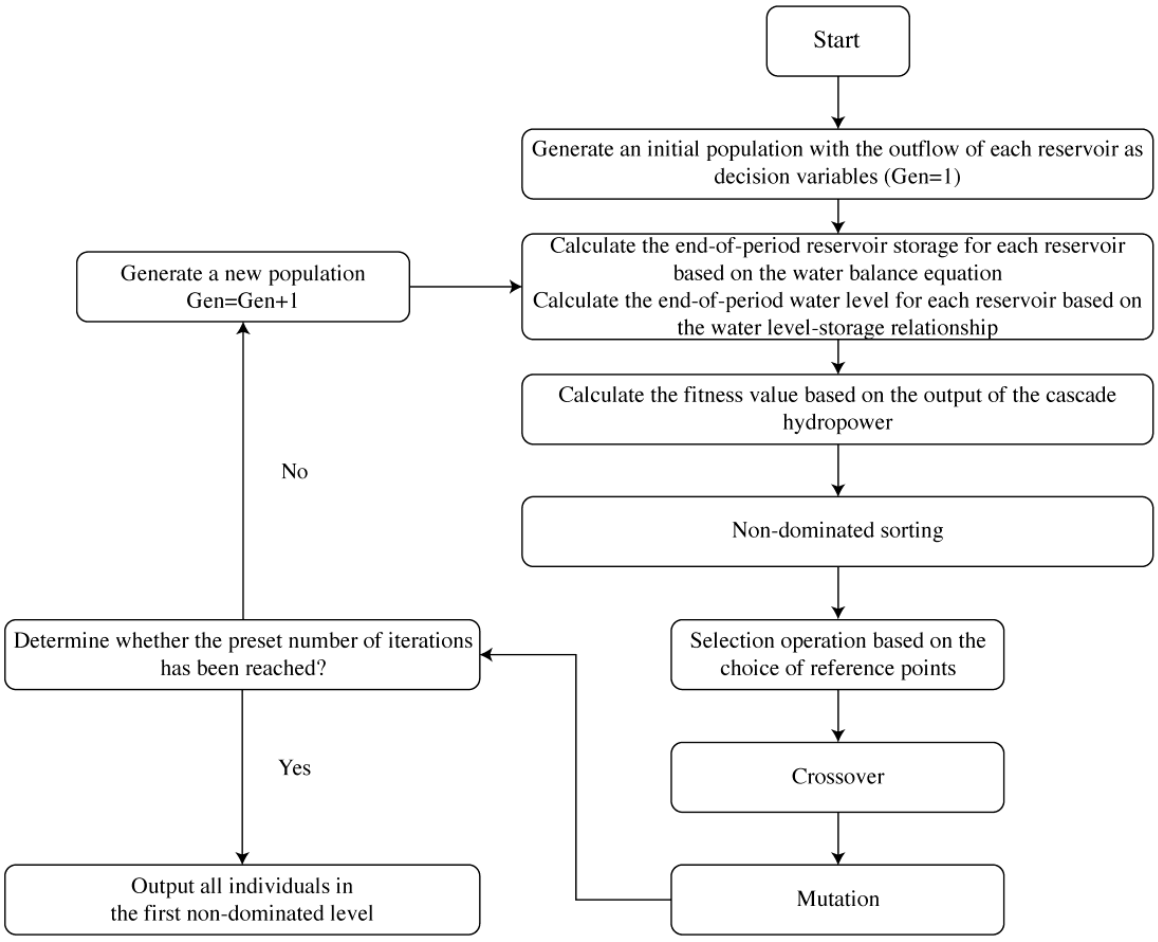

Figure 4. Process used to solve the long-term optimization scheduling model.

The NSGA-III was employed to resolve the long-term power generation optimization scheduling model and optimize the scheduling model of the hydro-PV hybrid system considering the short-term operational performance. The hyperparameters were set as follows: population size 200, crossover probability 0.90, mutation probability 0.05, and

number of iterations 5000. To mitigate the potential instability in the results of the intelligent algorithm, each typical year scenario was solved five times and all obtained non-dominated solutions were subjected to secondary non-dominated sorting. This process culminated in the determination of the overall Pareto front (or Pareto solution set).

2.3.2. Fuzzy Multi-Attribute Decision-Making

In multi-attribute decision making, the decision maker must consider multiple attributes or criteria simultaneously, each of which has a certain degree of uncertainty, incompleteness, and subjectivity. Fuzzy mathematics can better address these characteristics. Fuzzy multi-attribute decision-making refers to a decision-making problem in which multiple attributes are considered and fuzzy mathematical methods are used to comprehensively evaluate schemes. The best alternative scheme is then determined from a set of schemes, and the alternative schemes are comprehensively sorted [39]. We adopted the fuzzy multi-attribute decision-making method to screen the results of the multi-objective optimization scheduling model. A combination of subjective and objective weighting methods was used to determine the weight factors and avoid the subjectivity of the subjective weighting method and the one-sidedness of the objective weighting method [40]. As different attributes often have different physical meanings, they lead to inconsistencies in the dimensions of different attributes or significant differences in absolute values. Therefore, when making multi-attribute decisions, it is necessary to normalise the values of different attributes to facilitate comparison and sorting.

First, the membership degree of each non-inferior solution for each evaluation criterion (or objective function) was calculated. Equations (25) and (26) were used when the objective function was larger and smaller, respectively:

$$u_{ij} = (x_{ij} - x_{i,min})/(x_{i,max} - x_{i,min}) \tag{25}$$

$$u_{ij} = (x_{i,max} - x_{ij})/(x_{i,max} - x_{i,min}) \tag{26}$$

where u_{ij} is the relative membership degree of the ith criterion in the jth non-dominated solution (also referred to as scheme j), x_{ij} is the value of the ith criterion in scheme j, and $x_{i,max}$ and $x_{i,min}$ are the maximum and minimum values of the ith evaluation criterion, respectively.

Next, the normalised membership degree for each non-dominated solution (or scheme) was calculated based on its relative membership degree. The non-dominated solution with the largest normalised membership degree was considered the balanced solution for the multi-objective optimization scheduling model, as follows:

$$\lambda_j = \frac{\sum_{i=1}^{I} w_i \cdot u_{i,j}}{\sum_{i=1}^{I} \sum_{j=1}^{J} w_i \cdot u_{i,j}} \tag{27}$$

where J and I are the number of schemes and the number of evaluation criteria in the non-dominated solution set, respectively; w_i is the weight of the i-th criterion, with $\sum_{i=1}^{N} w_i = 1$, $0 \leq w_i \leq 1$; and λ_j is the normalised membership degree value for scheme j.

2.4. Case Study

2.4.1. Description of Study Region

The hydro-PV hybrid system investigated in this study is located in the Wu River Basin in southwestern China. The hybrid system includes four cascade hydropower plants in the Wu River Basin, namely Hongjiadu, Dongfeng, Suofengying, and Wujiangdu, as well as a centralised PV power station with an installed capacity of 1710 MW. As shown in Figure 5, hydropower and PV power are transformed and then centrally dispatched by the control centre before being connected to the main power grid. This study examined the hydro-PV hybrid system as a whole, focusing on its ability to supply power to the main

power grid and to participate in the peak load regulation of the main power grid. The main characteristic parameters of each hydropower station are listed in Table 1.

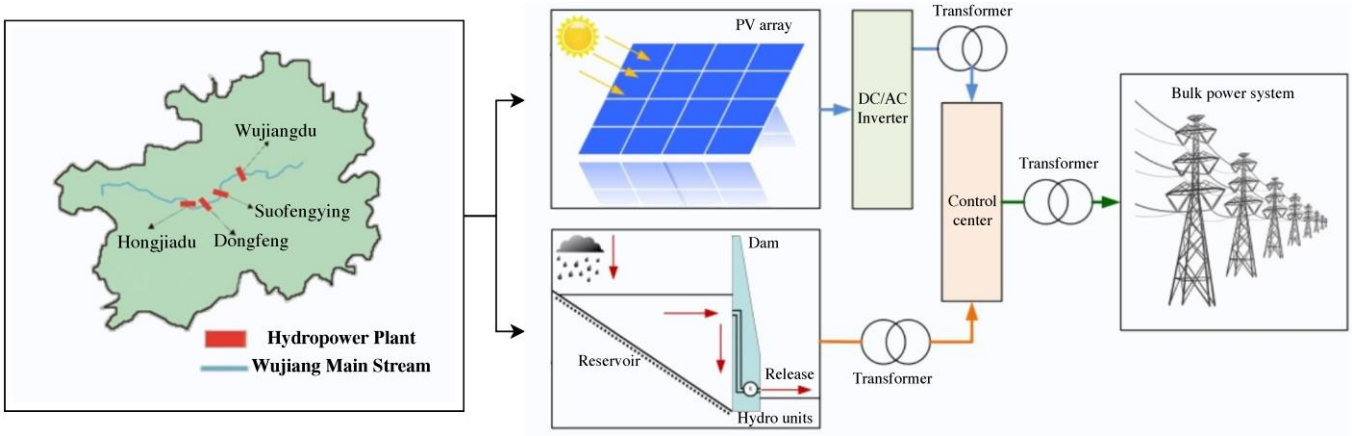

Figure 5. Locations of hydropower stations.

Table 1. Main characteristic parameters of the hydropower stations.

Hydropower Plant Name	Hongjiadu	Dongfeng	Suofengying	Wujiangdu
Installed capacity (MW)	600	695	600	1250
Design annual power generation (10^8 Kw h)	15.59	29.58	20.11	41.40
Power station output coefficient	8.50	8.35	8.50	8.17
Lower limit level for flood (m)	1138 (Jun~Aug), 1140	970	837	760
Dead water level (m)	1076	936	822	720
Regulating reservoir capacity (10^8 m^3)	33.61	4.90	0.67	13.60
Upper limit of discharge flow (m^3/s)	14.7	35.5	39.5	48.3
Lower limit of discharge flow (m^3/s)	3866	11,142	15,956	18,360

2.4.2. Settings and Input Data

(1) Typical day scenario

Short-term optimal scheduling requires the use of a series of typical day scenarios as inputs. According to the description in Section 2.2.1, typical day scenarios include three aspects: initial water level scenario setup, inflow scenario setup, and PV power output scenario setup.

For the initial water level scenario setup, for non-flood months (November to April of the following year), 10 sets of initial water level scenarios were taken in sequence according to the principle of uniform distribution from high to low water levels. For flood months (May to October), two additional scenarios exceeding the flood control limit water level were set based on the initial 10 scenarios.

For the inflow scenario setup, calculating the hydrological frequency of the daily average inflow/interval flow was mainly performed for Hongjiadu Reservoir. Based on the daily average inflow/interval flow data of the Wu River cascade reservoirs from July 1983 to June 2023, the fitting method of the hydrological frequency calculation was used to calculate the daily average inflow/interval flow data for 10%, 25%, 50%, 75%, and 90% of the five frequencies for each month.

For the PV power output scenario setup, this study was based on the hourly PV power output data of the study area from 2005 to 2016. The average value of the PV power output process for each month was calculated and used as the predicted PV power output process for each month. Based on the predicted PV power output process for each month, 100 sets of PV power output scenarios were generated using the Latin hypercube sampling method, and all 100 sets of scenarios were reduced to 10 sets using the K-means clustering method.

The predicted PV power output process and PV power output scenarios for all 12 months are shown in Figure 6.

In summary, for the non-flood months, there were 10 × 5 × 10 = 500 typical day scenarios; for flood months, there were 12 × 5 × 10 = 600 typical day scenarios.

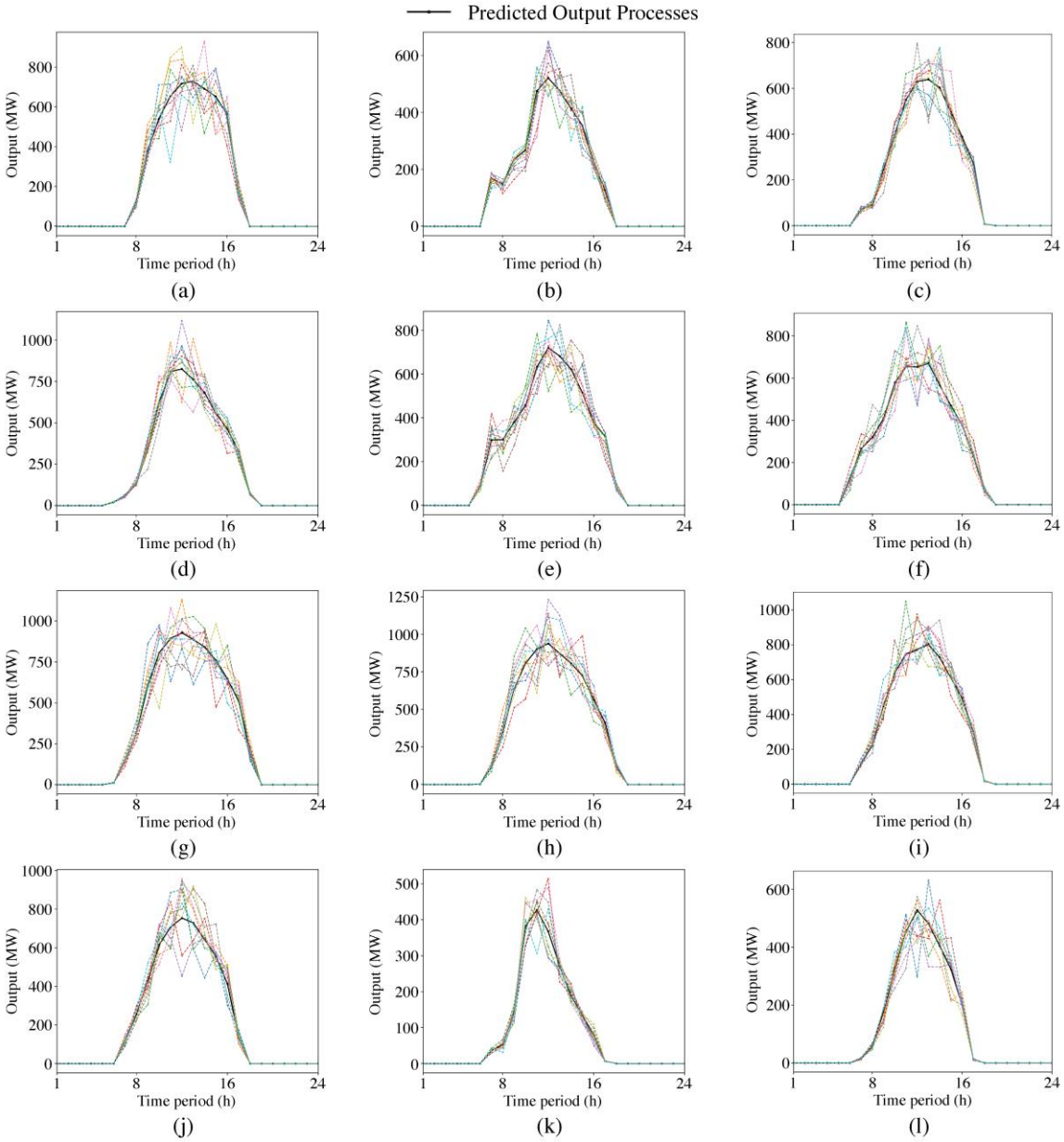

Figure 6. Predicted PV power output processes and PV power output scenarios for (**a**) January, (**b**) February, (**c**) March, (**d**) April, (**e**) May, (**f**) June, (**g**) July, (**h**) August, (**i**) September, (**j**) October, (**k**) November, and (**l**) December (coloured series represent multiple prediction processes generated for a single output process).

(2) Input data for the long-term optimization model

A hydrological frequency analysis was conducted using monthly inflow data of the four reservoirs from 1965 to 2020. Three typical types of inflow data were selected from the dataset: wet, normal, and dry. The PV power output was calculated using the formula from the PVWatts™ software Version 5 (https://pvwatts.nrel.gov/, accessed on 1 October 2023) by the National Renewable Energy Laboratory. The monthly output of the PV power station was calculated based on the measured solar radiation intensity and temperature

data in the study area. The inflow and PV power output processes for the three years are shown in Figure 7.

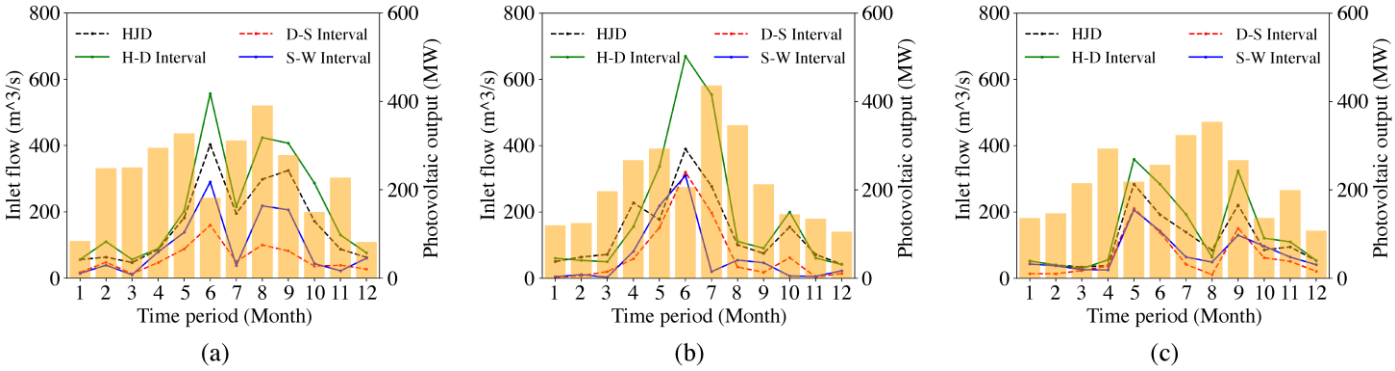

Figure 7. Inflow and PV power output processes for three typical years: (**a**) wet year, (**b**) normal year, and (**c**) dry year.

(3) Comparative scheme

To compare and verify the advantages of using the long-term optimal scheduling model in the hydro-PV hybrid power generation system considering the short-term operational performance, the following three scheduling models were set as comparative schemes. Model 1: optimization scheduling model of the hydro-PV hybrid system with the maximum power generation as the optimization criterion, representing a case that does not consider the short-term operational performance. Model 2: optimization scheduling model of the hydro-PV hybrid system with the maximum on-grid electricity as the optimization criterion. This considers the potential loss of on-grid electricity due to electricity curtailment, but it ignores power shortages and does not focus on the impact of electricity curtailment penalties. Model 3: optimization scheduling model of the hydro-PV hybrid system considering the short-term operational performance (i.e., the optimization scheduling model established in Section 2.1 of this paper). The input data of the three optimization scheduling models were identical, and the differences between the models are listed in Table 2.

Table 2. Different long-term optimization scheduling models used in hydro-PV hybrid systems.

Optimization Model	Objective Function	Short-term Operational Performance Indicators Considered	Scheduling Auxiliary Functions Used
Model 1	Maximum power generation	/	/
Model 2	Maximum on-grid electricity	Electricity curtailment	$f^{ec}(\cdot)$
Model 3	Maximum on-grid electricity, Minimise electricity curtailment volume, Minimise power shortage volume	Electricity curtailment, Power shortage	$f^{ec}(\cdot), f^{ps}(\cdot)$

3. Results and Discussion

3.1. Results of Scheduling Auxiliary Function Extraction

To investigate the characteristics of the hydro-PV hybrid system under different long-term scheduling periods, we extracted the scheduling auxiliary functions for each month. The complete set of 12 auxiliary scheduling functions is shown in Figure 8. There were certain differences in the scheduling of auxiliary functions across various months, which were determined by varying water and PV resource endowments in different months. The scheduling auxiliary functions for most months exhibited a U-shape, indicating that when the hydropower output was relatively low, the short-term operational performance indicators were relatively poor. These indicators were optimised as the hydropower output increased, but they deteriorated again when hydropower output was excessively high.

Based on the scheduling auxiliary functions, it was possible to quantitatively characterise various short-term operational performance indicators of the hydro-PV hybrid system within the long-term scheduling model.

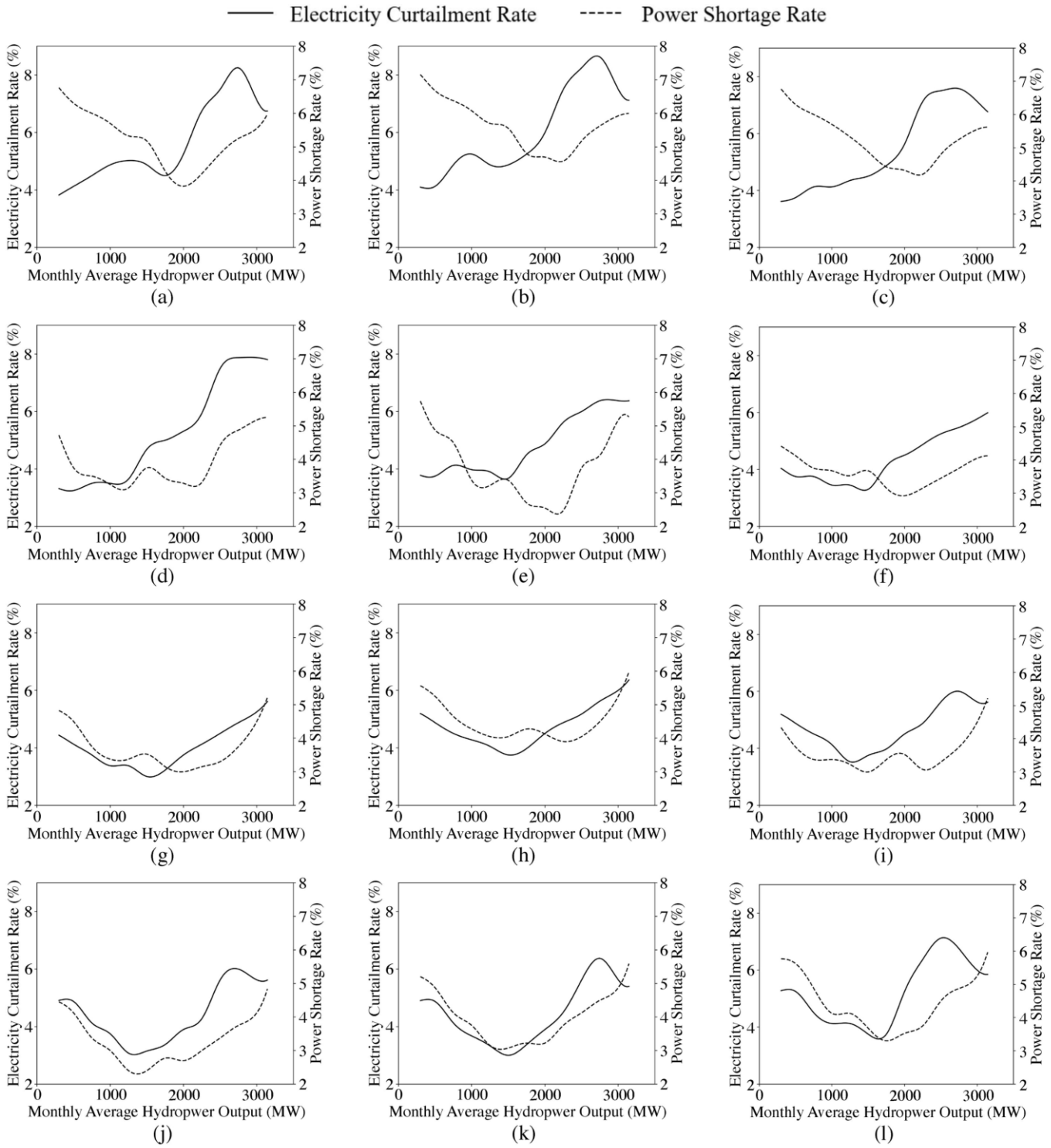

Figure 8. Scheduling auxiliary function graphs: (**a**) January, (**b**) February, (**c**) March, (**d**) April, (**e**) May, (**f**) June, (**g**) July, (**h**) August, (**i**) September, (**j**) October, (**k**) November, and (**l**) December.

The scheduling auxiliary functions in this study were extracted based on the multi-scenario analysis of short-term scheduling; however, some assumptions and simplifications were inevitably made during the scenario setting process, leading to certain errors in the

scheduling auxiliary functions. To validate the reliability of the scheduling auxiliary functions, simulation scheduling was conducted for a period of one month, and the simulated results of the short-term operational performance indicators were compared with the outcomes calculated based on the scheduling auxiliary functions. The following procedure was used.

Simulation scheduling first provided multiple boundary conditions for the beginning and end water levels of the cascade reservoirs for a certain month, based on which the monthly water consumption was calculated; the water consumption was evenly distributed to each day, and the beginning and end water levels as well as the power generation schedule curve for each day were calculated. Subsequently, a short-term optimization scheduling model (as shown in Section 2.2.2) was solved for each day, based on which the average hydropower output, average electricity curtailment rate, and average power shortage rate were calculated. Finally, the average hydropower output obtained from the simulation scheduling was substituted into the two scheduling auxiliary functions to calculate the corresponding short-term operational performance indicators and to assess the differences in the short-term operational performance indicators obtained by the two methods.

For the verification calculation, we selected a certain month as an example. First, five sets of different boundary conditions for the beginning and end water levels of the cascade reservoirs were obtained (see Table 3). The average hydropower output and short-term operational performance indicators obtained by the two calculation methods under different boundary conditions are shown in Table 4. The results show that under different long-term hydropower output levels, the differences between the short-term operational performance indicators derived from the simulation scheduling of the hydro-PV hybrid system and those calculated based on the scheduling auxiliary functions are generally small, indicating that the scheduling auxiliary functions in this paper are reliable.

Table 3. Initial and final water levels corresponding to different boundary conditions (unit: m).

Hydropower Plant Name	Hongjiadu		Dongfeng		Suofengying		Wujiangdu	
Boundary Condition Number	Beginning Water Level	End Water Level	Beginning Water Level	End Water Level	Beginning Water Level	End Water Level	Beginning Water Level	End Water Level
1	1095	1090	950	952.5	833	833	745	750
2	1095	1095	950	952.5	833	833	745	750
3	1095	1100	950	952.5	833	833	745	750
4	1095	1102.5	950	952.5	833	833	745	750
5	1095	1105	950	952.5	833	833	745	750

Table 4. Average hydropower output and short-term operational performance indicators obtained using two calculation methods under different boundary conditions.

Boundary Condition Number	Average Hydropower Output (MW)	Electricity Curtailment Rate (%)		Power Shortage Rate (%)	
		Simulation Scheduling	Scheduling Auxiliary Functions	Simulation Scheduling	Scheduling Auxiliary Functions
1	1752	3.68	4.00	3.10	2.75
2	1491	3.57	3.74	3.15	3.01
3	1202	3.54	3.62	3.20	3.17
4	1044	3.56	3.51	3.24	3.22
5	882	3.69	3.51	3.45	3.35

3.2. Analysis of Pareto Solution Sets

The NSGA-III was employed to solve the optimization scheduling model of the hydro-PV hybrid system considering short-term operational performance (i.e., Model 3). For the analysis of the competitive and collaborative relationships among the different optimization objectives, the boundaries of each objective within the three Pareto solution sets are summarised in Table 5.

Table 5. Boundaries of each objective in the three Pareto solution sets.

Typical Year	On-Grid Electricity (10^8 kW h)			Electricity Curtailment Volume (10^8 kW h)			Power Shortage Volume (10^8 kW h)		
	Best Value	Worst Value	Range	Best Value	Worst Value	Range	Best Value	Worst Value	Range
Wet	136.388	119.439	16.950	5.531	6.895	1.364	5.198	5.776	0.578
Normal	122.178	102.755	19.423	4.897	6.950	2.054	4.881	5.484	0.603
Dry	100.142	98.525	1.617	4.093	4.596	0.503	4.015	4.450	0.435

In general, if a scheduling scheme provided higher on-grid electricity generation, its corresponding short-term operational performance indicators tended to be poorer. Taking the Pareto front of the long-term power generation optimization scheduling for a wet year as an example, when the on-grid electricity generation target of the complementary system achieved its optimal value of 13.6388 billion kW·h, the electricity curtailment reached 689 million kW·h, which was very close to the worst value among all solutions of 689.5 million kW·h, and the power shortage volume was 574.2 million kW·h, which was also close to the poorest value of 577.6 million kW·h. At the optimal electricity curtailment value of 553.1 million kW·h, the on-grid electricity generation and power shortage volume of the complementary system were 121.63 billion kW·h and 567.2 million kW·h, respectively, which were in the middle to slightly inferior range of their respective values in the non-dominated solution set. Similarly, when the power shortage volume reached its optimal value, the on-grid electricity generation of the complementary system and electricity curtailment were close to their worst values. These results indicate a competitive relationship between the long-term power generation objectives and the short-term operational performance objectives of the hydro-PV hybrid system, as well as among different short-term operational performance objectives, with optimizing one objective tending to deteriorate the values of the other objective functions. However, there were variations in the impacts of different objectives on others during optimization. Therefore, in multi-objective optimization, it is beneficial to optimise the objectives that have a smaller negative impact on other objectives. To further analyse the competitive or collaborative relationships between the objectives, the three-dimensional Pareto front was projected onto the corresponding two-dimensional plane along each coordinate axis and the relationships between on-grid electricity, electricity curtailment and power shortage volume for the three typical years were plotted (Figure 9).

There was a negative correlation between electricity curtailment and power shortage volume in the different Pareto fronts, and this correlation was more pronounced in wet and dry years. This negative correlation indicates that reducing electricity curtailment lead to an increase in power shortage volume (i.e., a deterioration of the indicators), reflecting a competitive relationship. The lighter-coloured data points in the upper-right corner indicate that achieving higher on-grid electricity generation comes at the cost of poorer short-term operational performance indicators, reflecting the competitiveness between long-term power generation objectives and short-term operational performance objectives. The distribution of solutions with higher on-grid electricity being more uniform in the vertical direction and mostly concentrated on the right side in the horizontal direction suggests that achieving higher on-grid electricity led to a significant increase in power shortage volume, while the impact on electricity curtailment was not significant. That is, there was intense

competition between electricity curtailment and power shortage volume and between on-grid electricity and power shortage volume, while the competition between on-grid electricity and electricity curtailment was less intense. In summary, the three objectives of on-grid electricity, electricity curtailment, and power shortage volume in a hydro-PV hybrid system are competitive, and it is not possible to optimise them simultaneously. It is therefore necessary to select scientific scheduling schemes to achieve a balance between different optimization objectives.

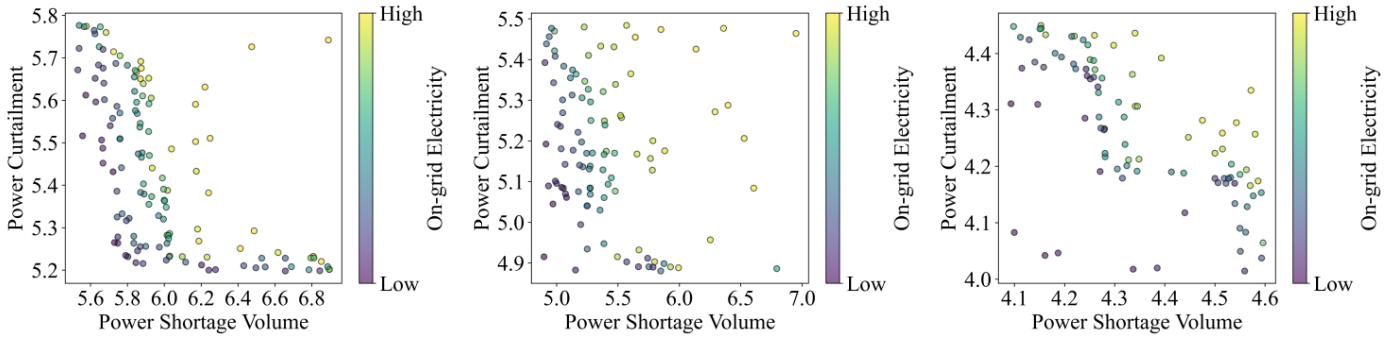

Figure 9. Projection graphs of Pareto solution sets for three typical years: (**a**) wet year, (**b**) normal year, and (**c**) dry year.

3.3. Analysis of Long-Term Model Optimization Results

3.3.1. Scheduling Results of Different Optimization Models

Different optimization models were used to solve the optimal scheduling process of the three typical years. Table 6 summarises the scheduling results under various optimization models for each typical year. Comparing the scheduling results of the various optimization models, it is evident that Model 1 achieved the maximum power generation, but its electricity curtailment was also relatively large. This resulted in a situation in which the on-grid electricity of Model 1 was less than that of Model 2, thereby reflecting the limitations of ignoring the short-term operational performance in long-term scheduling. Model 3, which considered both short-term operational performance indicators, slightly underperformed Models 2 and 1 in terms of on-grid electricity. However, its electricity curtailment and power shortage volumes were lower, thus balancing the long-term power generation objectives with the short-term operational performance objectives.

Table 6. Scheduling results for each typical year under different optimization models.

Typical Year	Objective Function	Power Generation (10^8 kW h)	On-Grid Electricity (10^8 kW h)	Electricity Curtailment Volume (10^8 kW h)	Power Shortage Volume (10^8 kW h)
Wet	Model 1	143.462	135.939	7.522	5.749
	Model 2	143.278	136.388	6.900	5.742
	Model 3	141.184	135.154	6.030	5.233
Normal	Model 1	129.407	121.179	8.228	5.810
	Model 2	128.372	122.081	6.290	5.271
	Model 3	127.094	121.213	5.880	5.176
Dry	Model 1	106.303	99.989	6.313	4.932
	Model 2	104.714	100.142	4.572	4.335
	Model 3	104.291	99.950	4.341	4.306

3.3.2. Comparison and Analysis of the Scheduling Process

To reveal the deep-seated reasons for the performance improvements in Models 2 and 3, the output processes corresponding to each optimization model were analysed, as

shown in Figures 10–12. By integrating Table 6 with Figures 10–12, it can be seen that the differences in annual power generation and annual on-grid electricity between the different optimization methods were not significant, whereas the differences in the output processes were pronounced. This is because different optimization methods redistribute energy between different periods to optimise their respective objective functions. The examination of scheduling auxiliary function in the present study shows that the correlations between hydropower output at different times and short-term operational performance indicators vary; therefore, optimization models that consider short-term operational performance will sacrifice some power generation as a cost of generating more electricity during periods with lower electricity curtailment and power shortage rates. Furthermore, the output process of the complementary system in Model 3 was more stable, followed by that in Model 2, whereas the output process of the complementary system in Model 1 was less stable. This is because, compared to Model 1, Models 2 and 3 considered the short-term operational performance of the complementary system and redistributed energy across different periods to "guide" the hydropower output during most periods towards improving short-term operational performance indicators, while also making the monthly output processes more stable throughout the year. In addition, the guiding effect of Model 3 was stronger than that of Model 2. Overall, the scheduling processes of Models 2 and 3, which consider the short-term operational performance, differed significantly from those of Model 1, indicating that considering the short-term operational performance significantly changed the power generation scheduling of the hydro-PV hybrid system. Thus, traditional cascade hydropower generation scheduling theories may not apply to the power generation scheduling of hydro-PV hybrid systems after the integration of large-scale PV power generation.

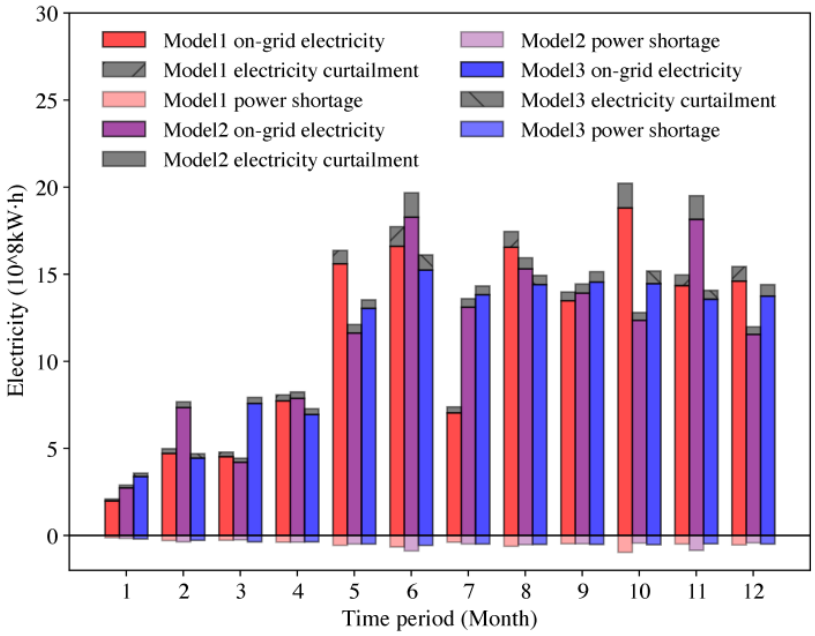

Figure 10. Comparison of power output processes for different optimization models in a wet year.

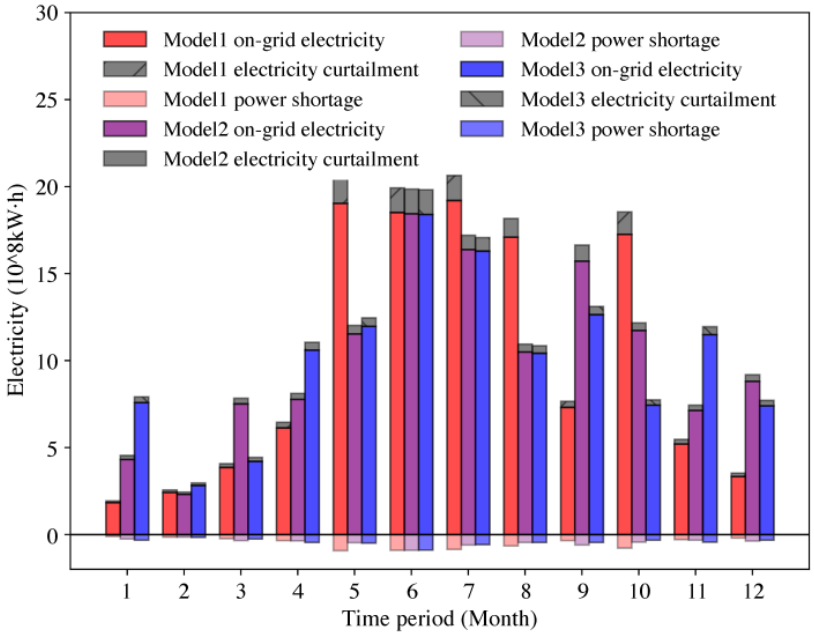

Figure 11. Comparison of power output processes for different optimization models in a normal year.

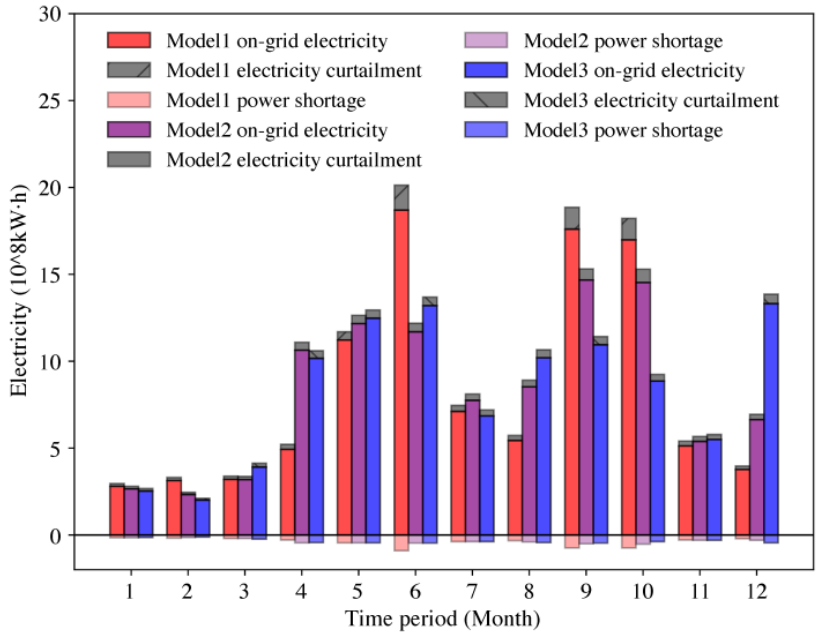

Figure 12. Comparison of power output processes for different optimization models in a dry year.

Among the four reservoirs, Hongjiadu Reservoir, which is located upstream of the cascade reservoir system, had the highest regulatory capacity. Therefore, we discuss the similarities and differences in energy allocation among the different optimization models by analysing the water-level change process of Hongjiadu Reservoir. As shown in Figure 13, during wet and normal years, Model 1 raised the water level of Hongjiadu Reservoir from January to May to ensure higher electrical energy output during the flood season, while Models 2 and 3 increased the hydropower output from January to May while reducing the hydropower output during the flood season. This confirms that considering short-term operational performance leads to a redistribution of energy across different periods. Due to reasons such as less available water, in the dry year, Model 1 did not exhibit the characteristic of "raising the water level during the dry season and generating more electricity during the flood season"; however, it did still redistribute energy due to

considering short-term operational performance. For example, from January to May in a dry year, the water-level change processes of Models 2 and 3, which considered short-term operational performance, were very similar but significantly different from that of Model 1.

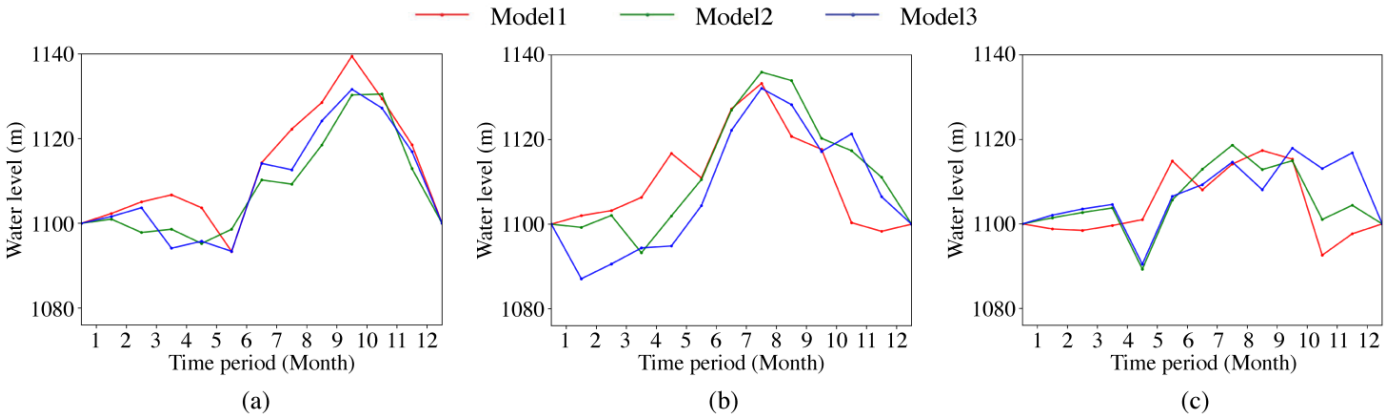

Figure 13. Water level change process at Hongjiadu under different optimization models: (**a**) wet year, (**b**) normal year, and (**c**) dry year.

3.3.3. Impact of Electricity Curtailment

To analyse the impact of electricity curtailment on the long-term scheduling of the complementary system, the scheduling results of Models 1 and 2 were compared. When the input data for three typical years (wet, normal, and dry) were used as model inputs, considering electricity curtailment, the power generation of the complementary system decreased by 0.13%, 0.80%, and 1.49%, respectively. However, owing to the reduction in electricity curtailment, on-grid electricity increased by 0.33%, 0.74%, and 1.53%, respectively. The presence of electricity curtailment implies that achieving the maximum power generation for the hydro-PV hybrid system does not necessarily equate to achieving the maximum on-grid electricity. Considering electricity curtailment in the long-term scheduling of the hydro-PV hybrid system can effectively reduce the amount of curtailed electricity and increase the on-grid electricity of the complementary system. Furthermore, as the input data changed from wet to dry years, the proportion of power generation decreased for Model 2 compared to Model 1, but the proportion of on-grid electricity increased for Model 2. The improvement effect brought about by considering electricity curtailment for complementary system scheduling was best in dry years and worst in wet years.

April of a dry year was taken as an example to conduct a detailed analysis of the improvement effect brought about by considering electricity curtailment for complementary system scheduling. The output of Model 2 was significantly higher than that of Model 1 (Figure 14); however, the electricity curtailment rate was similar to that of Model 1. The scheduling auxiliary function for April showed that when the hydropower output was not higher than 1250 MW, the electricity curtailment rate remained at a relatively stable level; however, when the hydropower output exceeded 1250 MW, the electricity curtailment rate rapidly increased. The hydropower output value for the month in Model 2 was achieved before the electricity curtailment rate rapidly increased with the growth of the hydropower output, achieving as high an output as possible while avoiding a sharp deterioration in the short-term operational performance indicators.

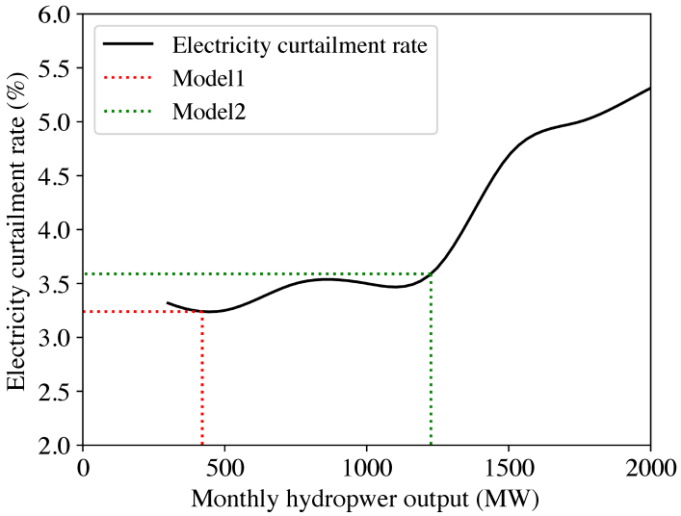

Figure 14. Comparison of hydropower output and electricity curtailment rate in April in a dry year.

3.3.4. Impact of Power Shortages

The above analysis indicates that Model 1 lags Model 2 in all aspects, implying that long-term optimization scheduling that considers electricity curtailment is more effective than scheduling that does not. In addition to considering electricity curtailment, Model 3 also considers power shortages. To provide a detailed analysis of the impact of power shortages on the long-term scheduling of the complementary system, the scheduling results of Models 2 and 3 were compared. When three typical years (wet, normal, and dry) were used as model input data, compared with Model 2, the complementary system on-grid electricity of Model 3 decreased by 0.90%, 0.71%, and 0.19%; electricity curtailment decreased by 12.61%, 6.52%, and 5.05%; and power shortage volume decreased by 8.86%, 1.80%, and 0.67%, respectively. Overall, considering power shortages in the long-term scheduling of the hydro-PV hybrid system can effectively reduce the power shortage volume without significantly decreasing on-grid electricity. The improvement effect of considering power shortages on the complementary system scheduling was best in wet years and similar in normal and dry years.

3.3.5. Comprehensive Impact of Short-Term Operational Performance

Finally, the scheduling results of Models 1 and 3 were compared to analyse the comprehensive impact of considering the short-term operational performance on the long-term scheduling of the complementary system. When the three typical years (wet, normal, and dry) were used as model input data, compared to Model 1, the complementary system on-grid electricity of Model 3 decreased by 0.58%, −0.03% (i.e., in the normal year, Model 3's on-grid electricity was slightly higher than Model 1), and 0.04%; electricity curtailment decreased by 19.84%, 28.54%, and 31.23%; and the power shortage volume decreased by 8.98%, 10.91%, and 12.69%, respectively. This indicates that considering the short-term operational performance in the long-term scheduling of the hydro-PV hybrid system led to a slight loss in on-grid electricity; however, there were significant improvements in the performance of PV utilization and avoidance of power shortages.

As illustrated in Figure 15, Model 3 had a lower hydropower output than Model 1 in November. However, by examining the scheduling auxiliary function graph, it is evident that, during wet years, Model 3 deliberately reduced the hydropower output for that month, corresponding to a more favourable short-term operational performance indicator. Similarly, in Figure 16, during a normal year, Model 3 increased the hydropower output, aiming to achieve a better short-term operational performance indicator. By integrating the comparative analysis of the scheduling results under different optimization models for each typical year, it is evident that Model 3 achieved a balance between the long-term power generation objectives and short-term operational performance targets. This was

accomplished by reallocating energy across different periods. Model 3 ensured that there was no significant reduction in the on-grid electricity of the complementary system while "guiding" the hydropower output during most periods to align with the improvement of short-term operational performance indicators.

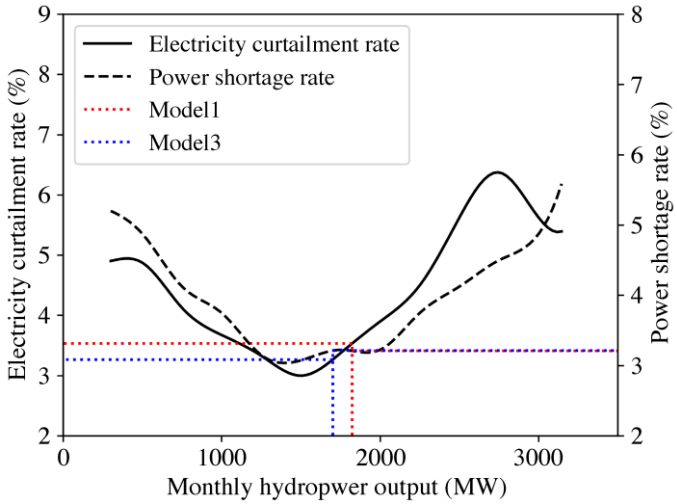

Figure 15. Comparison of hydropower output with short-term operational performance indicators in November in a wet year.

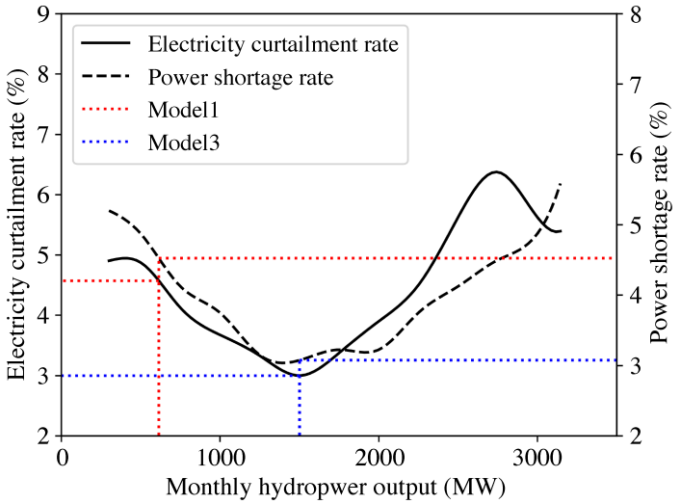

Figure 16. Comparison of hydropower output with short-term operational performance indicators in November in a normal year.

4. Conclusions

The main conclusions were as follows:

(1) The short-term operational performance indicators of the hydro-PV hybrid system were correlated with the long-term hydropower output and this correlation varied across different scheduling periods. The electricity curtailment rate and power shortage rate indicators generally gradually decreased with increasing hydropower output; however, excessive hydropower output can lead to increases in these indicators.

(2) Considering electricity curtailment in the long-term scheduling of a hydro-PV hybrid system effectively reduced the amount of curtailed electricity and increased the on-grid electricity of the complementary system.Similarly, considering power shortages in the long-term scheduling can effectively reduce the amount of power shortages without significantly decreasing on-grid electricity.Moreover, the improvement brought

about by considering the short-term operational performance for the scheduling of the complementary system was sensitive to water abundance conditions.

(3) Considering the short-term operational performance in the long-term scheduling of the hydro-PV hybrid system led to a slight loss in on-grid electricity; however, it significantly improved the performance of PV utilization and avoidance of power shortages, achieving a balance between long-term power generation objectives and short-term operational performance objectives. In the typical wet, normal, and dry years, compared with the optimization model that did not consider short-term operational performance, the optimization model that considered short-term operational performance resulted in minimal losses in on-grid electricity (0.58% loss, 0.03% increase, and 0.04% loss), while reducing electricity curtailment by 19.84%, 28.54%, and 31.23%, respectively, and power shortage volume by 8.98%, 10.91%, and 12.69%, respectively.

The findings indicate that the proposed model addresses the traditional limitations of long-term scheduling that often neglect the coordination between photovoltaic power consumption and water resource utilization in river basins. These findings provide decision support for hydropower scheduling in the context of large-scale photovoltaic power integration.

Admittedly, our current research results have certain limitations that need to be addressed. In the present study, short-term optimization outcomes influenced long-term scheduling, whereas long-term optimization outcomes did not impact short-term scheduling, so that the interconnection between the two types of scheduling was disregarded. To fully exploit the advantages of applying short-term optimization results to long-term scheduling, future research could consider establishing a bidirectional coupled optimization scheduling model for the hydro-PV hybrid system to make the simulated operation process of the hydro-PV hybrid system more realistic. A potential bidirectional coupled optimization scheduling model could involve conducting short-term scheduling of the complementary system based on boundary conditions provided by long-term scheduling, examining the impact of uncertainties in each short-term scheduling period (such as photovoltaic power output) on its short-term operational performance, and carrying out rolling optimization calculations. Additionally, this study focused on the changes to long-term scheduling of the complementary system by considering the short-term operational performance, and the established model differed from reality to some extent. The resulting issues include an overemphasis on typical years, an insufficient consideration of the complexity of real-world implementation, highly simplified assumptions about hydropower operations, a limited scope of performance indicators, neglecting other common power sources (such as wind power), and a lack of economic analysis. These issues all need to be refined and strengthened in future research.

Author Contributions: Conceptualization, W.Y. and Z.S.; methodology, W.Y. and Z.S.; software, Z.S.; validation, Z.S.; formal analysis, Z.S.; investigation, W.Y.; resources, W.Y. and Z.S.; data curation, W.Y., and Z.S.; writing—original draft preparation, Z.S.; writing—review and editing, Z.S.; visualization, Z.S.; supervision, W.Y. All authors have read and agreed to the published version of the manuscript.

Funding: This research received no external funding.

Data Availability Statement: The original contributions presented in the study are included in the article, further inquiries can be directed to the corresponding author.

Conflicts of Interest: The authors declare no conflicts of interest.

References

1. Yalew, S.G.; van Vliet, M.T.H.; Gernaat, D.E.H.J.; Ludwig, F.; Miara, A.; Park, C.; Byers, E.; De Cian, E.; Piontek, F.; Iyer, G.; et al. Impacts of climate change on energy systems in global and regional scenarios. *Nat. Energy* **2020**, *5*, 794–802. [CrossRef]
2. Wang, Q.; Guo, J.; Li, R. Better renewable with economic growth without carbon growth: A comparative study of impact of turbine, photovoltaics, and hydropower on economy and carbon emission. *J. Clean. Prod.* **2023**, *426*, 10. [CrossRef]

3. Hu, Y.; Duan, F.; Wang, H.; Li, C.; Zhang, R.; Tang, B. Pathways for regions to achieve carbon emission peak: New insights from the four economic growth poles in China. *Sci. Total Environ.* **2024**, *907*, 167979. [CrossRef] [PubMed]
4. Guo, J.; Chen, Z.; Meng, J.; Zheng, H.; Fan, Y.; Ji, L.; Wang, X.; Liang, X. Picturing China's photovoltaic energy future: Insights from CMIP6 climate projections. *Renew. Sustain. Energ. Rev.* **2024**, *189*, 13. [CrossRef]
5. Zhao, M.; Yu, R.; Chang, C.; Bao, D.; Mei, A.; Liu, Y.; Wang, N. Effect of sand and dust shading on the output characteristics of solar photovoltaic modules in desertification areas. *Energies* **2023**, *16*, 7910. [CrossRef]
6. Zhao, X.; Ren, Y.; Sha, Y.; Zhang, L.; Hou, S.; Xiao, F.; Chen, F.; Chen, S.; He, K.; Luo, L.; et al. Research on the impact of hydro-PV complementary system operation on power grid based on new energy consumption. *Math. Probl. Eng.* **2022**, *2022*, 1–11. [CrossRef]
7. Zhu, Z.; Wang, L.; Wang, X.; Jiang, C.; Zhou, S.; Gong, K. Complementary operations of multi-renewable energy systems with pumped storage. *CSEE J. Power Energy Syst.* **2023**, *9*, 1866–1880. [CrossRef]
8. Michael, N.E.; Bansal, R.C.; Ismail, A.A.A.; Elnady, A.; Hasan, S. Optimized energy management for photovoltaic/wind hybrid micro-grid using energy storage solution. *Int. J. Modell. Simul.* **2023**, *18*, 1–18. [CrossRef]
9. Li, Z.M.; Xu, Y.; Feng, X.; Wu, Q.W. Optimal Stochastic Deployment of Heterogeneous Energy Storage in a Residential Multienergy Microgrid With Demand-Side Management. *IEEE Trans. Ind. Inform.* **2021**, *17*, 991–1004. [CrossRef]
10. Wang, Y.; Shi, P.; Zeng, Z.; Li, X.; Zhou, B. Coordinated operation of PV and cascaded hydropower considering the power grid security constraints. In Proceedings of the 2021 International Conference on Power System Technology (POWERCON), Haikou, China, 8–9 December 2021; pp. 1035–1039. [CrossRef]
11. Jurasz, J.; Beluco, A.; Canales, F.A. The impact of complementarity on power supply reliability of small scale hybrid energy systems. *Energy* **2018**, *161*, 737–743. [CrossRef]
12. Zheng, X.; Qu, K.; Lv, J.; Li, Z.; Zeng, B. Addressing the Conditional and Correlated Wind Power Forecast Errors in Unit Commitment by Distributionally Robust Optimization. *IEEE Trans. Sustain. Energy* **2021**, *12*, 944–954. [CrossRef]
13. Cao, H.; Qiu, J.; Zuo, H.; Li, F. A long-term operational scheme for hybrid hydro-photovoltaic (PV) systems that considers the uncertainties in reservoir inflow and solar radiation based on scenario trees. *Water Resour. Manag.* **2023**, *37*, 5379–5398. [CrossRef]
14. Li, H.; Liu, P.; Guo, S.; Ming, B.; Cheng, L.; Yang, Z. Long-term complementary operation of a large-scale hydro-photovoltaic hybrid power plant using explicit stochastic optimization. *Appl. Energy* **2019**, *238*, 863–875. [CrossRef]
15. Lu, N.; Wang, G.Y.; Su, C.; Ren, Z.; Peng, X.; Sui, Q. Medium- and long-term interval optimal scheduling of cascade hydropower-photovoltaic complementary systems considering multiple uncertainties. *Appl. Energy* **2024**, *353*, 17. [CrossRef]
16. Li, F.; Wu, Z.; Wei, J.; Qiu, J. Long-term equilibrium operational plan for hydro-PV hybrid power system considering benefits, stability, and tolerance. *J. Water Resour. Plann. Manag.* **2020**, *146*, 10. [CrossRef]
17. Ming, B.; Liu, P.; Cheng, L. An integrated framework for optimizing large hydro-photovoltaic hybrid energy systems: Capacity planning and operations management. *J. Clean. Prod.* **2021**, *306*, 14. [CrossRef]
18. Wu, X.; Cheng, C.; Li, G.; Zhang, S. Research on long term typical day peak load regulation energy maximization model for hydropower systems. *J. Hydraul. Eng.* **2012**, *43*, 363–371. [CrossRef]
19. Cheng, Q.; Luo, P.; Liu, P.; Li, X.; Ming, B.; Huang, K.; Xu, W.; Gong, Y. Stochastic short-term scheduling of a wind-solar-hydro complementary system considering both the day-ahead market bidding and bilateral contracts decomposition. *Int. J. Electr. Power Energy Syst.* **2022**, *138*, 11. [CrossRef]
20. Cheng, Q.; Liu, P.; Cheng, L.; Ming, B.; Yang, Z.; Luo, X.; Xu, W.; Gong, L.; Zhang, Y. Underestimated climate change impacts on hydro-wind-photovoltaic complementary systems due to neglect of short-term features. *J. Hydrol.* **2023**, *626*, 13. [CrossRef]
21. Wang, F.; Xie, Y.; Xu, J. Reliable-economical equilibrium based short-term scheduling towards hybrid hydro-photovoltaic generation systems: Case study from China. *Appl. Energy* **2019**, *253*, 16. [CrossRef]
22. Park, S.; Kim, Y.; Ferrier, N.J.; Collis, S.M.; Sankaran, R.; Beckman, P.H. Prediction of solar irradiance and photovoltaic solar energy product based on cloud coverage estimation using machine learning methods. *Atmosphere* **2021**, *12*, 395. [CrossRef]
23. Yuan, W.; Wang, X.; Su, C.; Cheng, C.; Liu, Z.; Wu, Z. Stochastic optimization model for the short-term joint operation of photovoltaic power and hydropower plants based on chance-constrained programming. *Energy* **2021**, *222*, 15. [CrossRef]
24. Huang, K.D.; Liu, P.; Ming, B.; Kim, J.S.; Gong, Y. Economic operation of a wind-solar-hydro complementary system considering risks of output shortage, power curtailment and spilled water. *Appl. Energy* **2021**, *290*, 13. [CrossRef]
25. Wang, X.; Mei, Y.; Kong, Y.; Lin, Y.; Wang, H. Improved multi-objective model and analysis of the coordinated operation of a hydro-wind-photovoltaic system. *Energy* **2017**, *134*, 813–839. [CrossRef]
26. Eltamaly, A.M. Musical chairs algorithm for parameters estimation of PV cells. *Sol. Energy* **2022**, *241*, 601–620. [CrossRef]
27. Hu, Y.; Wang, J.; Liang, J.; Yu, K.; Song, H.; Guo, Q.; Yue, C.; Wang, Y. A self-organizing multimodal multi-objective pigeon-inspired optimization algorithm. *Sci. China-Inf. Sci.* **2019**, *62*, 17. [CrossRef]
28. Zhang, S.; Qiu, G.; Liu, Y.; Ding, L.; Shui, Y. Data-driven distributionally robust optimization-based coordinated dispatching for cascaded hydro-PV-PSH combined system. *Electronics* **2024**, *13*, 667. [CrossRef]
29. Xianyu, H.; Huang, X.; Li, X.; Li, D.; Zhang, Y.; Xu, C. Risk scheduling strategy based on hydro-PV-load module hierarchical cooperative searching. *Power Syst. Technol.* **2023**, *47*, 908–917. [CrossRef]
30. Guo, X.; Zheng, L.; Li, G.; Cui, Q.; Ji, S.; Jiang, J.; Ming, B. Optimal sizing of photovoltaic power generation for integration into a large hydropower plant. *China Rural. Water Hydropower* **2023**, *12*, 273–279+288. [CrossRef]

31. Ming, B.; Li, Y.; Liu, P.; Wang, Y.; Ma, C.; Huang, Q. Long-term optimal operation of hydro-solar hybrid energy systems nested with short-term energy curtailment risk. *J. Hydraul. Eng.* **2021**, *52*, 712–722. [CrossRef]
32. Cerejo, A.; Mariano, S.; Carvalho, P.M.S.; Calado, M.R.A. Hydro-wind optimal operation for joint bidding in day-ahead market: Storage efficiency and impact of wind forecasting uncertainty. *J. Mod. Power Syst. Clean Energy* **2020**, *8*, 142–149. [CrossRef]
33. Cheng, Q.; Liu, P.; Feng, M.Y.; Cheng, L.; Ming, B.; Luo, X.; Liu, W.; Xu, W.; Huang, K.; Xia, J. Complementary operation with wind and photovoltaic power induces the decrease in hydropower efficiency. *Appl. Energy* **2023**, *339*, 10. [CrossRef]
34. Guo, Y.; Ming, B.; Huang, Q.; Wang, Y.; Zheng, X.; Zhang, W. Risk-averse day-ahead generation scheduling of hydro-wind-photovoltaic complementary systems considering the steady requirement of power delivery. *Appl. Energy* **2022**, *309*, 15. [CrossRef]
35. Lu, L.; Yuan, W.; Su, C.; Wang, P.; Cheng, C.; Yan, D.; Wu, Z. Optimization model for the short-term joint operation of a grid-connected wind-photovoltaic-hydro hybrid energy system with cascade hydropower plants. *Energy Conv. Manag.* **2021**, *236*, 12. [CrossRef]
36. Derepasko, D.; Witing, F.; Peñas, F.J.; Barquín, J.; Volk, M. Towards adaptive water management-optimizing river water diversion at the basin scale under future environmental conditions. *Water* **2023**, *15*, 3289. [CrossRef]
37. Deb, K.; Jain, H. An evolutionary many-objective optimization algorithm using reference-point-based nondominated sorting approach, Part I: Solving problems with box constraints. *IEEE Trans. Evol. Comput.* **2014**, *18*, 577–601. [CrossRef]
38. Zhao, Y.; Wang, J.; Huang, X.; Sun, Z. A multi-objective scheduling strategy of CH-PV-Wind-PS based on an improved hybrid intelligent algorithm. In Proceedings of the International Conference on Power System Technology (POWERCON), Haikou, China, 8–9 December 2021; Volume 2021, pp. 1147–1154. [CrossRef]
39. Zuo, Q.; Guo, J.; Ma, J.; Cui, G.; Yang, R.; Yu, L. Assessment of regional-scale water resources carrying capacity based on fuzzy multiple attribute decision-making and scenario simulation. *Ecol. Indic.* **2021**, *130*, 10. [CrossRef]
40. Yang, W.; Xue, M.; Wang, Y.; Long, T.; Deng, S.; Deng, B.; Fang, N. Evaluation of enterprise green mine construction based on DPSIR model. *Int. J. Environ. Res. Public Health* **2023**, *20*, 4932. [CrossRef]

Disclaimer/Publisher's Note: The statements, opinions and data contained in all publications are solely those of the individual author(s) and contributor(s) and not of MDPI and/or the editor(s). MDPI and/or the editor(s) disclaim responsibility for any injury to people or property resulting from any ideas, methods, instructions or products referred to in the content.